

An Assumed Strain Solid Shell Element Formulation with Transversely Quadratic Displacement

K. Lee¹ and S.W. Lee²

Abstract: A geometrically nonlinear assumed strain formulation is used to develop a nine-node solid shell element with quadratic displacement through the thickness. The transversely quadratic element allows direct use of the constitutive equations developed for three-dimensional solids, which is convenient when material nonlinearity is involved. The nodal degrees of freedom associated with the quadratic terms in the assumed displacement through the thickness are statically condensed out at the element level. The results of numerical tests conducted on selected example problems demonstrate the validity and effectiveness of the present approach. For the cases involving linear elastic material, the differences between the present element and the solid shell element with linear displacement through the thickness are negligible.

Keyword: geometrically nonlinear, assumed strain, transversely quadratic, solid shell element

1 Introduction

Computational modeling of shell structures has been an active research area for the last decades. Several kinds of finite elements have been developed for shell analysis such as degenerated solid shell element [Ahmad, Irons and Zienkiewicz (1970)], shell theory-based element [Simo and Rifai (1990)] and three-dimensional (3D) solid shell element [Ausserer and Lee (1988), Kim and Lee (1988)]. For an extensive literature survey on shell finite elements, one may refer to Yang, Saigal, Masoud and Kapania (2000) and Arciniega and Reddy (2007). Alternatively, meshless approaches have been used for shell analyses by Atluri and Zhu (1998) and Sladek, Sladek, Wen and Aliabadi (2006). In the finite element modeling of various shell models, one needs to pay a close attention to their salient features and limitations in order to avoid computational errors. In the present work, we

¹ Assistant Research Scientist, University of Maryland, College Park, MD, USA

² Professor, University of Maryland, College Park, MD, USA

briefly mention how differently constitutive equations have been incorporated into these shell elements depending upon selected assumptions in their kinematics of deformation.

A shell element formulation that allows using the fully 3D constitutive law is attractive for applications involving materially nonlinear deformation. However, for the 'inextensible' shell approach that does not allow changes in the thickness, the plane stress assumption is unavoidable, complicating its materially nonlinear formulation, as shown by Tonkovic, Soric and Skozrit (2008). The 'extensible' shell approach that allows changes in the thickness can be more versatile if one can avoid the plane stress assumption in the constitutive equations. One example would be direct application of elastoplasticity theories developed for 3D solids [Han, Rajendran and Atluri (2005), Liu (2005)] to elastoplastic shell analysis using the full Newton-Raphson iteration. Within the context of the extensible shell approach, the linear displacement assumption in the thickness direction has been dominantly used. For the case of linear elastic materials, the linear assumption together with a constitutive law modified to describe the thin shell behavior is adequate for analysis of shell structures [Ausserer and Lee (1988), Kim and Lee (1988)]. However, it can be still inconvenient to adopt constitutive laws for materially nonlinear formulation. Therefore, various approaches including the seven parameter model have been developed to overcome this difficulty without introducing undue numbers of additional degrees of freedom. Notable examples are the works reported by Sainsour (1995), Parisch (1995), Hauptmann and Schweizerhof (1998), El-Abbasi and Meguid (2000), Vu-Quoc and Tan (2003), Klinkel, Gruttmann and Wagner (2006), and Kulikov and Plotnikova (2008). In addition, several higher order shell elements incorporating higher-order displacement assumptions through the thickness to describe the nonlinear transverse strains have been developed by Tabiei and Tanov (2000), Balah and Al-Ghamedy (2002), Basar, Hanskotter and Schwab (2003), and Arciniega and Reddy (2007) to name a few.

For the meshless-based formulation, Soric, Li, Jarack and Atluri (2004) and Li, Soric, Jarack, and Atluri (2005) introduced an approach with the hierarchical quadratic interpolation over the thickness. Subsequently, Jarack, Soric and Hoster (2007) used two separate interpolation schemes: a quadratic interpolation in the thickness direction to avoid the undesired thickness locking and the moving-least-square higher-order interpolation in the in-plane directions. Their solid-shell based kinematics allowed the use of 3D constitutive models.

The solid shell approach that treats the shell simply as a three-dimensional solid should naturally facilitate the use of constitutive equations developed for 3D solids. Moreover, the solid shell approach allows changes in the thickness and does not use any rotational angles in the kinematics of deformation, enabling large load incre-

ments for geometrically nonlinear analysis, [Park, Cho, and Lee (1995) and Lee, Cho and Lee (2002)]. However, for the existing assumed strain solid shell elements, the displacement has been assumed to be linear through the thickness. Accordingly, it is still necessary to modify the 3D constitutive equations in a manner consistent with the behavior of thin shell structures [Ausserer and Lee (1988), Kim and Lee (1988)]. The assumed strain formulation has been combined with the solid shell approach to alleviate the transverse shear locking and the inplane rigidity (or membrane) locking at the element level. For various assumed strain approaches to alleviate the element locking, one may refer to Lee and Pian (1978), Rhiu and Lee (1987), Kim and Lee (1988), and Park and Lee (1995).

In this study, a nine-node assumed strain solid shell element with quadratic displacement through the thickness is presented. This approach, initially introduced by Lee and Lee (2001), allows direct use of the constitutive equations developed for three-dimensional solids. Moreover, for thin shells, the nodal degrees of freedom associated with the quadratic terms in the assumed displacement through the thickness can be statically condensed out at the element level, under the premise that the strain energy associated with these degrees of freedom (DOF) is negligible. Accordingly, the present approach does not introduce any additional degrees of freedom at the global level. The assumed strain formulation is used to avoid the element locking. Numerical tests are conducted on selected example problems involving linear elastic material to demonstrate the validity and effectiveness of the present approach, via comparing the present solid shell element with the existing assumed strain solid shell element with linear displacement through the thickness.

2 Finite Element Formulation

A transversely quadratic solid shell element formulation is developed based on the total Lagrangian description that employs the Green strain and the second Piola-Kirchhoff stress, in conjunction with the assumed strain formulation.

2.1 Element geometry and kinematics of deformation

Figure 1 shows the reference surface of a nine-node solid shell element placed at the midsurface.

For the solid shell element, the geometry of the element can be expressed as follows:

$$\mathbf{x} = \mathbf{x}_0 + \zeta \frac{t}{2} \mathbf{a}_3 \tag{1}$$

where \mathbf{x}_0 is the position vector of a point on the shell mid-surface ($\zeta = 0$), ζ is a parental coordinate in the thickness direction, t is the shell thickness and \mathbf{a}_3 is a unit

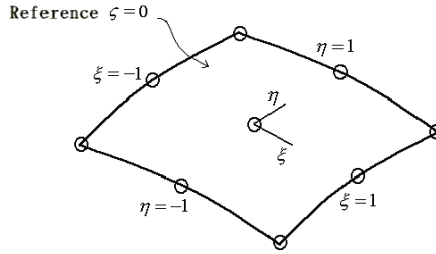


Figure 1: The reference surface of the nine-node solid shell element

vector in the thickness direction. The geometry of the element can be expressed in terms of nodal values as follows:

$$\mathbf{x} = \sum_{i=1}^n N_i(\xi, \eta)(\mathbf{x}_0)_i + \zeta \sum_{i=1}^n N_i(\xi, \eta) \left(\frac{t}{2} \mathbf{a}_3\right)_i \quad (2)$$

where n is the number of element nodes and $N_i, (\mathbf{x}_0)_i$ is the mapping function and the position vector for the i^{th} node, respectively. Note that the mapping function is expressed in terms of the parental coordinates ξ and η .

For the transversely linear solid shell element, we assume that the displacement varies linearly along the thickness direction such that

$$\mathbf{u} = \mathbf{u}_0 + z\mathbf{u}_1 = \mathbf{u}_0 + \zeta \frac{t}{2} \mathbf{u}_1 \quad (3)$$

where \mathbf{u}_0 is the displacement vector of a point on the mid-surface and z is equal to $\zeta \frac{t}{2}$. For the transversely linear shell element with the kinematics of deformation expressed in equation (3), the constitutive equation developed for three-dimensional solids must be modified to properly represent shell behavior via avoiding the so-called thickness locking.

Alternatively, in order to construct a shell element model that allows direct use of three-dimensional constitutive equations, one may introduce transversely quadratic displacement such that

$$\mathbf{u} = \mathbf{u}_0 + z\mathbf{u}_1 + z^2\mathbf{u}_2 \quad (4)$$

The assumed displacement vector can be expressed in terms of nodal values as follows:

$$\mathbf{u} = \sum_{i=1}^n N_i(\mathbf{u}_0)_i + \zeta \sum_{i=1}^n N_i \left(\frac{t}{2} \mathbf{u}_1\right)_i + \zeta^2 \sum_{i=1}^n N_i \left(\left(\frac{t}{2}\right)^2 \mathbf{u}_2\right)_i \quad (5)$$

For a nine-node element, the shape function N_i for the i^{th} node is a bi-quadratic function of ξ and η . Accordingly, the displacement vector is consistently quadratic with respect to the parental coordinates (ξ , η and ζ). Also, one may note that, in contrast to the degenerated solid shell approach, no rotational angles are used in this approach.

For geometrically nonlinear analysis, the unknown displacement vector \mathbf{u} can be written in terms of the displacement $^{(n)}\mathbf{u}$ at the known state (n) and its increment $\Delta\mathbf{u}$ as

$$\mathbf{u} = ^{(n)}\mathbf{u} + \Delta\mathbf{u} \quad (6)$$

Using equation (4), one can express the incremental displacement vector as

$$\Delta\mathbf{u} = \Delta\mathbf{u}_0 + z\Delta\mathbf{u}_1 + z^2\Delta\mathbf{u}_2 \quad (7)$$

Equation (7) can be written in an expanded form as

$$\begin{Bmatrix} \Delta u \\ \Delta v \\ \Delta w \end{Bmatrix} = \begin{Bmatrix} \Delta u_0 \\ \Delta v_0 \\ \Delta w_0 \end{Bmatrix} + z \begin{Bmatrix} \Delta u_1 \\ \Delta v_1 \\ \Delta w_1 \end{Bmatrix} + z^2 \begin{Bmatrix} \Delta u_2 \\ \Delta v_2 \\ \Delta w_2 \end{Bmatrix} \quad (8)$$

2.2 Strain fields

One may assume that the displacement-dependent strain vector $\bar{\boldsymbol{\epsilon}}$ is quadratic in ζ as

$$\bar{\boldsymbol{\epsilon}} = \bar{\boldsymbol{\epsilon}}_0 + \zeta\bar{\boldsymbol{\epsilon}}_1 + \zeta^2\bar{\boldsymbol{\epsilon}}_2 \quad (9)$$

where the over-bar is used for displacement-dependent quantities in this paper. Its incremental form is obtained using equation (6) and the strain-displacement relations can be written symbolically as follows:

$$\begin{aligned} \bar{\boldsymbol{\epsilon}} = & ^{(n)}\bar{\boldsymbol{\epsilon}}_0 + \Delta\bar{\boldsymbol{\epsilon}}_0 + \Delta\bar{\mathbf{h}}_0 \\ & + \zeta(^{(n)}\bar{\boldsymbol{\epsilon}}_1 + \Delta\bar{\boldsymbol{\epsilon}}_1 + \Delta\bar{\mathbf{h}}_1) \\ & + \zeta^2(^{(n)}\bar{\boldsymbol{\epsilon}}_2 + \Delta\bar{\boldsymbol{\epsilon}}_2 + \Delta\bar{\mathbf{h}}_2) \end{aligned} \quad (10)$$

where $\Delta\bar{\boldsymbol{\epsilon}}_{0,1,2}$ and $\Delta\bar{\mathbf{h}}_{0,1,2}$ are the incremental displacement-dependent strain vectors that are linear and quadratic in $\Delta\mathbf{u}$, respectively. Introducing the assumed displacement, incremental strain vectors in equation (10) that are linear in $\Delta\mathbf{u}$ can be expressed in matrix form as follows:

$$\begin{aligned} \Delta\bar{\boldsymbol{\epsilon}}_0 &= \mathbf{B}_0(\xi, \eta)\Delta\mathbf{q}_e \\ \Delta\bar{\boldsymbol{\epsilon}}_1 &= \mathbf{B}_1(\xi, \eta)\Delta\mathbf{q}_e \\ \Delta\bar{\boldsymbol{\epsilon}}_2 &= \mathbf{B}_2(\xi, \eta)\Delta\mathbf{q}_e \end{aligned} \quad (11)$$

where the incremental element DOF vector $\Delta \mathbf{q}_e$ consists of the nine DOFs at each node as

$$\Delta \mathbf{q}_e = \begin{Bmatrix} (\Delta u_0, \Delta v_0, \Delta w_0, \Delta u_1, \Delta v_1, \Delta w_1, \Delta u_2, \Delta v_2, \Delta w_2)_1^T \\ \vdots \\ (\Delta u_0, \Delta v_0, \Delta w_0, \Delta u_1, \Delta v_1, \Delta w_1, \Delta u_2, \Delta v_2, \Delta w_2)_9^T \end{Bmatrix} \quad (12)$$

For thin shells $\Delta u_2, \Delta v_2, \Delta w_2$ at nodes can be statically condensed out at the element level under the premise that the strain energy associated with these degrees of freedom is negligible.

Shell elements based on the assumed displacement alone suffer from element locking. An assumed strain formulation uses an independently assumed strain field to alleviate the element locking [Lee and Pian (1978)]. In general the independently assumed strain vector may be expressed to be quadratic in ζ as

$$\boldsymbol{\varepsilon} = \boldsymbol{\varepsilon}_0 + \zeta \boldsymbol{\varepsilon}_1 + \zeta^2 \boldsymbol{\varepsilon}_2 \quad (13)$$

Element locking is associated with the ζ -independent part of the strain. Accordingly, for the present element, an assumed strain field is introduced only for ζ -independent strain vector such that

$$\boldsymbol{\varepsilon} = \boldsymbol{\varepsilon}_0 + \zeta \bar{\boldsymbol{\varepsilon}}_1 + \zeta^2 \bar{\boldsymbol{\varepsilon}}_2 \quad (14)$$

Note that the strain vectors $\boldsymbol{\varepsilon}_1$ and $\boldsymbol{\varepsilon}_2$ in equation (13) are replaced by the displacement-dependent counterparts. The selection of a proper assumed strain field is vital to the element performance. The independently assumed vector $\boldsymbol{\varepsilon}_0$ can be divided into two parts as

$$\boldsymbol{\varepsilon}_0 = \boldsymbol{\varepsilon}_0^L + \boldsymbol{\varepsilon}_0^H \quad (15)$$

where $\boldsymbol{\varepsilon}_0^L$ is the lower-order part selected to alleviate locking and $\boldsymbol{\varepsilon}_0^H$ is the higher-order part introduced to suppress undesirable spurious kinematic modes. For the transversely quadratic nine-node solid shell element, the lower-order part is assumed bilinear in ξ and η as follows:

$$\begin{aligned} \varepsilon_{0xx}^L &= \alpha_1 + \alpha_2 \xi + \alpha_3 \eta + \alpha_4 \xi \eta \\ \varepsilon_{0yy}^L &= \alpha_5 + \alpha_6 \xi + \alpha_7 \eta + \alpha_8 \xi \eta \\ \varepsilon_{0zz}^L &= \alpha_9 + \alpha_{10} \xi + \alpha_{11} \eta + \alpha_{12} \xi \eta \\ \varepsilon_{0xy}^L &= \alpha_{13} + \alpha_{14} \xi + \alpha_{15} \eta + \alpha_{16} \xi \eta \\ \varepsilon_{0yz}^L &= \alpha_{17} + \alpha_{18} \xi + \alpha_{19} \eta + \alpha_{20} \xi \eta \\ \varepsilon_{0zx}^L &= \alpha_{21} + \alpha_{22} \xi + \alpha_{23} \eta + \alpha_{24} \xi \eta \end{aligned} \quad (16)$$

where x, y are the local coordinates tangent to the shell midsurface while z is normal to the midsurface. The details on construction of the local orthogonal coordinate system have been described by Park and Lee (1995). The lower order part alone triggers spurious kinematic modes. Accordingly, a higher-order part $\boldsymbol{\varepsilon}_0^H$ is chosen as follows to suppress the undesirable spurious kinematic modes:

$$\begin{aligned}
 \varepsilon_{0xx}^H &= \alpha_{25} \xi \eta^2 \\
 \varepsilon_{0yy}^H &= \alpha_{26} \xi^2 \eta \\
 \varepsilon_{0zz}^H &= 0 \\
 \varepsilon_{0xy}^H &= 0 \\
 \varepsilon_{0yz}^H &= \alpha_{27} \xi^2 \eta \\
 \varepsilon_{0zx}^H &= \alpha_{28} \xi \eta^2
 \end{aligned} \tag{17}$$

Note that twenty eight parameters from α_1 to α_{28} are used to express the assumed strain field. The ζ -independent assumed strain vector can be symbolically written in matrix form as

$$\boldsymbol{\varepsilon}_0 = \mathbf{P}_0 \boldsymbol{\alpha}_0 \tag{18}$$

where $\mathbf{P}_0(\xi, \eta)$ is the assumed strain shape function (matrix) and $\boldsymbol{\alpha}_0$ is a vector of the assumed strain parameters whose entries are $\alpha_{1\sim 28}$.

Then, equation (14) can be rewritten symbolically as follows:

$$\boldsymbol{\varepsilon} = \mathbf{P}_0(\xi, \eta) \boldsymbol{\alpha}_0 + \zeta \bar{\boldsymbol{\varepsilon}}_1 + \zeta^2 \bar{\boldsymbol{\varepsilon}}_2 \tag{19}$$

For geometrically nonlinear formulation, the unknown strain vector $\boldsymbol{\varepsilon}$ can be expressed as

$$\boldsymbol{\varepsilon} = {}^{(n)}\boldsymbol{\varepsilon} + \Delta \boldsymbol{\varepsilon} \tag{20}$$

where the incremental strain vector is expressed as

$$\Delta \boldsymbol{\varepsilon} = \Delta \boldsymbol{\varepsilon}_0 + \zeta \Delta \bar{\boldsymbol{\varepsilon}}_1 + \zeta^2 \Delta \bar{\boldsymbol{\varepsilon}}_2 \tag{21}$$

with

$$\Delta \boldsymbol{\varepsilon}_0 = \mathbf{P}_0(\xi, \eta) \Delta \boldsymbol{\alpha}_0 \tag{22}$$

Although the selection of the assumed strain field is carried out over a flat rectangular element, the same assumed strain field is used for a curved element using a local coordinate system, in which the z -axis is normal to the mid-surface and the x and y axes are tangent to the surface [Park and Lee, (1995)].

2.3 Compatibility

The independently assumed strain vector $\boldsymbol{\epsilon}_0$ can be related to the displacement-dependent strain vector $\bar{\boldsymbol{\epsilon}}_0$ via constructing a least square functional as

$$L = \frac{1}{2} \int_{V_e} (\boldsymbol{\epsilon}_0 - \bar{\boldsymbol{\epsilon}}_0)^T \mathbf{C} (\boldsymbol{\epsilon}_0 - \bar{\boldsymbol{\epsilon}}_0) dV \quad (23)$$

where \mathbf{C} , the matrix of linear elastic stiffness constants, serves as a weighting matrix. Alternatively, one may choose the identity matrix as the weighting matrix instead of the \mathbf{C} matrix. Substituting the strain terms in equations (10) and (18) into the above equation and setting

$$\frac{\partial L}{\partial \boldsymbol{\alpha}_0} = 0 \quad (24)$$

and neglecting the higher order terms in the incremental displacement vector leads to

$$\mathbf{H}_0 \Delta \boldsymbol{\alpha}_0 - \mathbf{F}_0 - \mathbf{G}_0 \Delta \mathbf{q}_e = 0 \quad (25)$$

where

$$\begin{aligned} \mathbf{F}_0 &= \int_{A_e} \mathbf{P}_0^T \mathbf{C}_0 ({}^{(n)}\bar{\boldsymbol{\epsilon}}_0 - {}^{(n)}\boldsymbol{\epsilon}_0) dA \\ \mathbf{G}_0 &= \int_{A_e} \mathbf{P}_0^T \mathbf{C}_0 \mathbf{B}_0 dA \\ \mathbf{H}_0 &= \int_{A_e} \mathbf{P}_0^T \mathbf{C}_0 \mathbf{P}_0 dA \end{aligned} \quad (26)$$

Note that the volume integral in equation (23) has been transformed to the area integral in equation (26). This can be done via assuming that the determinant J of the Jacobian matrix is linear in ζ as follows:

$$J(\xi, \eta, \zeta) = J_0(\xi, \eta) + \zeta J_1(\xi, \eta) \quad (27)$$

With the above assumption, one can introduce the following relation

$$dV = (1 + r\zeta) d\zeta dA \quad (28)$$

where $r(\xi, \eta) = J_1/J_0$. Equation (27) allows analytical integration through the shell thickness. The \mathbf{C}_0 matrix in equation (26) is obtained by analytically integrating the matrix of linear elastic stiffness through the thickness as

$$\mathbf{C}_0 = \int \mathbf{C} (1 + r\zeta) d\zeta \quad (29)$$

This feature is convenient in modeling of laminated composite structures [Kim and Lee (1988)].

From equation (25), one can determine the incremental vector of the assumed strain parameters as

$$\Delta\boldsymbol{\alpha}_0 = \mathbf{H}_0^{-1}(\mathbf{G}_0\Delta\mathbf{q}_e + \mathbf{F}_0) \quad (30)$$

Substituting equation (30) into equation (22), one can express the ζ -independent, incremental assumed strain vector as follows:

$$\Delta\boldsymbol{\varepsilon}_0 = \hat{\mathbf{B}}_0\Delta\mathbf{q}_e + \mathbf{P}_0\mathbf{H}_0^{-1}\mathbf{F}_0 \quad (31)$$

where

$$\hat{\mathbf{B}}_0 = \mathbf{P}_0\mathbf{H}_0^{-1}\mathbf{G}_0 \quad (32)$$

Accordingly, the incremental assumed strain vector can be rewritten as

$$\Delta\boldsymbol{\varepsilon} = \hat{\mathbf{B}}_0\Delta\mathbf{q}_e + \mathbf{P}_0\mathbf{H}_0^{-1}\mathbf{F}_0 + \zeta\Delta\bar{\boldsymbol{\varepsilon}}_1 + \zeta^2\Delta\bar{\boldsymbol{\varepsilon}}_2 \quad (33)$$

2.4 Equilibrium

For a solid in equilibrium,

$$\int_V \delta\bar{\boldsymbol{\varepsilon}}^T \boldsymbol{\sigma} dV - \delta W = 0 \quad (34)$$

where $\boldsymbol{\sigma}$ is the second Piola-Kirchhoff stress vector, $\delta\bar{\boldsymbol{\varepsilon}}$ is the virtual displacement-dependent strain vector, δW is the virtual work due to the applied load and V represents the volume of the undeformed configuration. The stress vector is related to the independent strain vector such that

$$\boldsymbol{\sigma} = \mathbf{C}\boldsymbol{\varepsilon} \quad (35)$$

The virtual displacement-dependent strain vector can be expressed in incremental form as

$$\begin{aligned} \delta\bar{\boldsymbol{\varepsilon}} &= \delta\bar{\boldsymbol{\varepsilon}}_0 + \zeta\delta\bar{\boldsymbol{\varepsilon}}_1 + \zeta^2\delta\bar{\boldsymbol{\varepsilon}}_2 \\ &= (\delta\bar{\boldsymbol{\varepsilon}}_0 + \delta\bar{\mathbf{h}}_0) + \zeta(\delta\bar{\boldsymbol{\varepsilon}}_1 + \delta\bar{\mathbf{h}}_1) + \zeta^2(\delta\bar{\boldsymbol{\varepsilon}}_2 + \delta\bar{\mathbf{h}}_2) \end{aligned} \quad (36)$$

where

$$\begin{aligned} \delta\bar{\boldsymbol{\varepsilon}}_0 &= \mathbf{B}_0(\xi, \eta)\delta\mathbf{q}_e \\ \delta\bar{\boldsymbol{\varepsilon}}_1 &= \mathbf{B}_1(\xi, \eta)\delta\mathbf{q}_e \\ \delta\bar{\boldsymbol{\varepsilon}}_2 &= \mathbf{B}_2(\xi, \eta)\delta\mathbf{q}_e \end{aligned} \quad (37)$$

Note that $\delta\bar{\mathbf{e}}_{0,1,2}$ does not include any $\Delta\mathbf{u}$ term while $\delta\bar{\mathbf{h}}_{0,1,2}$ is linear in $\Delta\mathbf{u}$. Using equations (20), (28), (35) and (36), one can rewrite the equilibrium equation in terms of area integration as follows:

$$\int_S [\delta\bar{\mathbf{e}}_0^T \quad \delta\bar{\mathbf{e}}_1^T \quad \delta\bar{\mathbf{e}}_2^T] \begin{Bmatrix} {}^{(n)}\mathbf{S}_0 + \Delta\mathbf{S}_0 \\ {}^{(n)}\mathbf{S}_1 + \Delta\mathbf{S}_1 \\ {}^{(n)}\mathbf{S}_2 + \Delta\mathbf{S}_2 \end{Bmatrix} dA - \delta W = 0 \quad (38)$$

where

$$\begin{aligned} {}^{(n)}\mathbf{S}_0 &= \int {}^{(n)}\boldsymbol{\sigma}(1+r\zeta)d\zeta \\ {}^{(n)}\mathbf{S}_1 &= \int {}^{(n)}\boldsymbol{\sigma}\zeta(1+r\zeta)d\zeta \\ {}^{(n)}\mathbf{S}_2 &= \int {}^{(n)}\boldsymbol{\sigma}\zeta^2(1+r\zeta)d\zeta \\ \Delta\mathbf{S}_0 &= \int \Delta\boldsymbol{\sigma}(1+r\zeta)d\zeta \\ \Delta\mathbf{S}_1 &= \int \Delta\boldsymbol{\sigma}\zeta(1+r\zeta)d\zeta \\ \Delta\mathbf{S}_2 &= \int \Delta\boldsymbol{\sigma}\zeta^2(1+r\zeta)d\zeta \end{aligned} \quad (39)$$

Using equation (36) and ignoring high-order terms in $\Delta\mathbf{u}$, one can rewrite the equilibrium equations as follows:

$$\begin{aligned} \int_S [\delta\bar{\mathbf{e}}_0^T \quad \delta\bar{\mathbf{e}}_1^T \quad \delta\bar{\mathbf{e}}_2^T] \begin{Bmatrix} {}^{(n)}\mathbf{S}_0 \\ {}^{(n)}\mathbf{S}_1 \\ {}^{(n)}\mathbf{S}_2 \end{Bmatrix} dA + \int_S [\delta\bar{\mathbf{h}}_0^T \quad \delta\bar{\mathbf{h}}_1^T \quad \delta\bar{\mathbf{h}}_2^T] \begin{Bmatrix} {}^{(n)}\mathbf{S}_0 \\ {}^{(n)}\mathbf{S}_1 \\ {}^{(n)}\mathbf{S}_2 \end{Bmatrix} dA \\ + \int_S [\delta\bar{\mathbf{e}}_0^T \quad \delta\bar{\mathbf{e}}_1^T \quad \delta\bar{\mathbf{e}}_2^T] \begin{Bmatrix} \Delta\mathbf{S}_0 \\ \Delta\mathbf{S}_1 \\ \Delta\mathbf{S}_2 \end{Bmatrix} dA - \delta W \approx 0 \end{aligned} \quad (40)$$

Dropping the higher order terms, the incremental stress in equation (39) can be expressed as

$$\Delta\boldsymbol{\sigma} = \mathbf{C}(\Delta\mathbf{e}_0 + \zeta\Delta\bar{\mathbf{e}}_1 + \zeta^2\Delta\bar{\mathbf{e}}_2) \quad (41)$$

At this stage, the virtual displacement-dependent strain vector $\delta\bar{\mathbf{e}}_0^T$ in the first and third terms of equation (40) is replaced by the virtual independent strain vector $\delta\mathbf{e}_0^T$

such that

$$\int_S [\delta \mathbf{e}_0^T \quad \delta \bar{\mathbf{e}}_1^T \quad \delta \bar{\mathbf{e}}_2^T] \begin{Bmatrix} {}^{(n)}\mathbf{S}_0 \\ {}^{(n)}\mathbf{S}_1 \\ {}^{(n)}\mathbf{S}_2 \end{Bmatrix} dA + \int_S [\delta \bar{\mathbf{h}}_0^T \quad \delta \bar{\mathbf{h}}_1^T \quad \delta \bar{\mathbf{h}}_2^T] \begin{Bmatrix} {}^{(n)}\mathbf{S}_0 \\ {}^{(n)}\mathbf{S}_1 \\ {}^{(n)}\mathbf{S}_2 \end{Bmatrix} dA + \int_S [\delta \mathbf{e}_0^T \quad \delta \bar{\mathbf{e}}_1^T \quad \delta \bar{\mathbf{e}}_2^T] \begin{Bmatrix} \Delta \mathbf{S}_0 \\ \Delta \mathbf{S}_1 \\ \Delta \mathbf{S}_2 \end{Bmatrix} dA - \delta W \approx 0 \quad (42)$$

Setting the virtual independent strain vector as

$$\delta \mathbf{e}_0 = \mathbf{P}_0 \delta \boldsymbol{\alpha}_0 \quad (43)$$

for the least square fit of $\delta \mathbf{e}_0$ with $\delta \bar{\mathbf{e}}_0$, one can show that

$$\delta \mathbf{e}_0 = \hat{\mathbf{B}}_0 \delta \mathbf{q}_e \quad (44)$$

Using equations (37) and (44), one can rewrite the first term in equation (42) symbolically as

$$\sum_e \delta \mathbf{q}_e^T \int [\hat{\mathbf{B}}_0^T {}^{(n)}\mathbf{S}_0 \quad \mathbf{B}_1^T {}^{(n)}\mathbf{S}_1 \quad \mathbf{B}_2^T {}^{(n)}\mathbf{S}_2] dA \equiv \sum_e \delta \mathbf{q}_e^T {}^{(n)}\mathbf{Q} \quad (45)$$

where ${}^{(n)}\mathbf{Q}$ is the load vector associated with the stress at state (n) . The second term in equation (42) can be expressed symbolically as

$$\int_S [\delta \bar{\mathbf{h}}_0^T \quad \delta \bar{\mathbf{h}}_1^T \quad \delta \bar{\mathbf{h}}_2^T] \begin{Bmatrix} {}^{(n)}\mathbf{S}_0 \\ {}^{(n)}\mathbf{S}_1 \\ {}^{(n)}\mathbf{S}_2 \end{Bmatrix} dA = \sum_e \delta \mathbf{q}_e^T \mathbf{K}_s \Delta \mathbf{q}_e \quad (46)$$

where \mathbf{K}_s is the stiffness matrix due to the stress at state (n) . Using equations (33), (37), (39) and (44), one can rewrite the third term in equations (42) as

$$\sum_e \delta \mathbf{q}_e^T \int [\hat{\mathbf{B}}_0^T \quad \mathbf{B}_1^T \quad \mathbf{B}_2^T] \begin{bmatrix} \mathbf{C}_0 & \mathbf{C}_I & \mathbf{C}_{II} \\ \mathbf{C}_I & \mathbf{C}_{II} & \mathbf{C}_{III} \\ \mathbf{C}_{II} & \mathbf{C}_{III} & \mathbf{C}_{IV} \end{bmatrix} \begin{Bmatrix} \hat{\mathbf{B}}_0 \\ \mathbf{B}_1 \\ \mathbf{B}_2 \end{Bmatrix} dA \Delta \mathbf{q}_e + \sum_e \delta \mathbf{q}_e^T \int [\hat{\mathbf{B}}_0^T \quad \mathbf{B}_1^T \quad \mathbf{B}_2^T] \begin{Bmatrix} \mathbf{C}_0 \\ \mathbf{C}_I \\ \mathbf{C}_{II} \end{Bmatrix} \mathbf{P}_0 dA \mathbf{H}_0^{-1} \mathbf{F}_0 \equiv \sum_e \delta \mathbf{q}_e^T (\mathbf{K}_B \Delta \mathbf{q}_e + \mathbf{Q}_0) \quad (47)$$

where

$$\begin{aligned}
 \mathbf{C}_0 &= \int \mathbf{C}(1+r\zeta)d\zeta \\
 \mathbf{C}_I &= \int \mathbf{C}\zeta(1+r\zeta)d\zeta \\
 \mathbf{C}_{II} &= \int \mathbf{C}\zeta^2(1+r\zeta)d\zeta \\
 \mathbf{C}_{III} &= \int \mathbf{C}\zeta^3(1+r\zeta)d\zeta \\
 \mathbf{C}_{IV} &= \int \mathbf{C}\zeta^4(1+r\zeta)d\zeta
 \end{aligned} \tag{48}$$

The virtual work due to the applied load in equation (42) can be expressed as

$$\sum \delta W_e \equiv \sum \delta \mathbf{q}_e^T \mathbf{Q}_{ext} \tag{49}$$

where \mathbf{Q}_{ext} is the load vector due to externally applied loads.

Finally, equation (42) leads to the equation for iterative analysis as

$$\sum \delta \mathbf{q}_e^T (\mathbf{K}_e \Delta \mathbf{q}_e - \Delta \mathbf{Q}_e) = 0 \tag{50}$$

where the element stiffness matrix and element load vector is as follows:

$$\begin{aligned}
 \mathbf{K}_e &= \mathbf{K}_s + \mathbf{K}_B \\
 \Delta \mathbf{Q}_e &= \mathbf{Q}_{ext} - {}^{(n)}\mathbf{Q} - \mathbf{Q}_0
 \end{aligned} \tag{51}$$

The DOF vector corresponding to quadratic displacement through the thickness direction is statically condensed out at the element level to maintain the number of element DOF at 54.

3 Numerical Tests

Several numerical tests are conducted to examine the performance of the new solid shell element in comparison with that of the existing nine-node solid shell element. Examples chosen are geometrically nonlinear plates and shells of simple geometries under static loading conditions. For convenience of presenting numerical results, the following designations are used for the new element and the existing element.

SHELL9-3D: a nine-node assumed strain solid shell element with quadratic displacement through the thickness direction and with fully 3D constitutive equations.

SHELL9: a nine-node assumed strain solid shell element with linear displacement through the thickness direction and with modified constitutive equations [Kim and Lee (1988), Park, Cho, and Lee (1995)]

It is well to mention that, as shown by Park and Lee (1995), the SHELL9 element passes patch tests carried out for flat plates under uniform tension and bending moment. The SHELL-3D is simply an element with more degrees of freedom added to the SHELL element in the thickness direction. Accordingly, it also passes the patch tests.

Also, it is to be noted that, for the SHELL9-3D element, all calculations are carried out using the version in which the degrees of freedom for the quadratic displacement through the thickness are eliminated at the element level.

3.1 A clamped square plate under a point force

A square plate shown in Fig. 2 is clamped on all edges. The length L of the plate is 2" and the thickness t is 0.002". The material is isotropic with a Young's modulus $E = 1.7472 \times 10^7$ psi and a Poisson's ratio $\nu = 0.3$. The plate is subjected to a transverse load at point C in Fig. 2. Due to the geometric and load symmetry, only one quarter of the plate is modeled using a uniform 4×4 mesh as shown in Fig. 2.

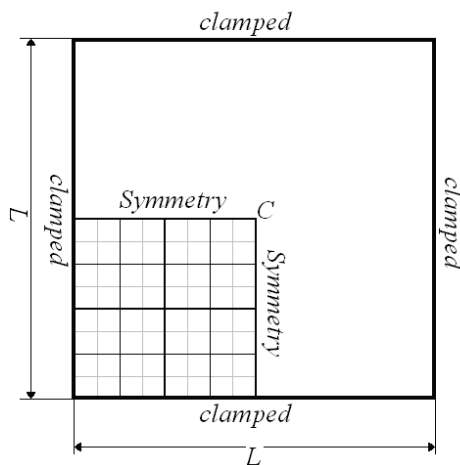


Figure 2: A clamped square plate

Geometrically nonlinear analysis is carried out using the SHELL9-3D and the SHELL9 elements. The results of the geometrically nonlinear analysis are shown in

Fig. 3 where the solution obtained by the SHELL9-3D element is almost identical to that by the SHELL9 element.

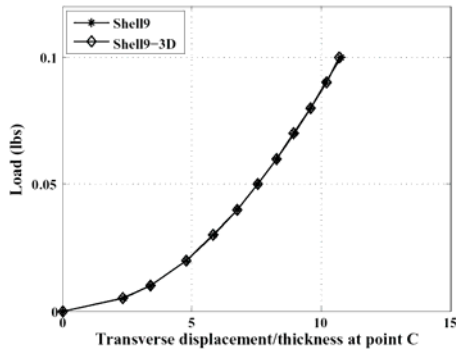


Figure 3: Load vs. transverse displacement/thickness at point C for $L/t=1000$

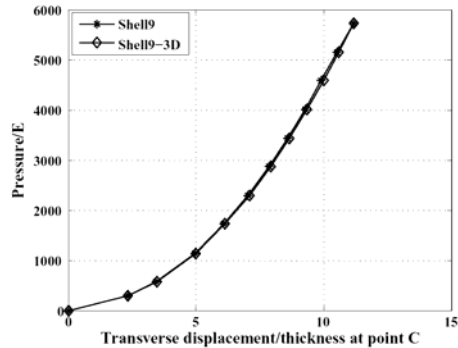


Figure 4: Pressure/E vs. transverse displacement/thickness at point C for $L/t=100$

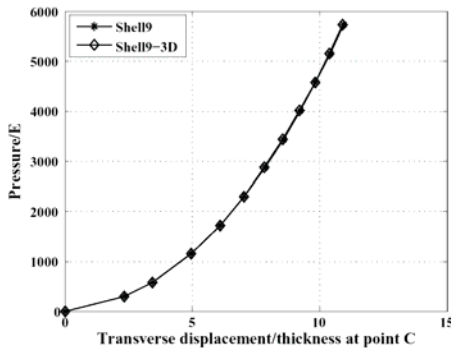


Figure 5: Pressure/E vs. transverse displacement/thickness at point C for $L/t=1000$

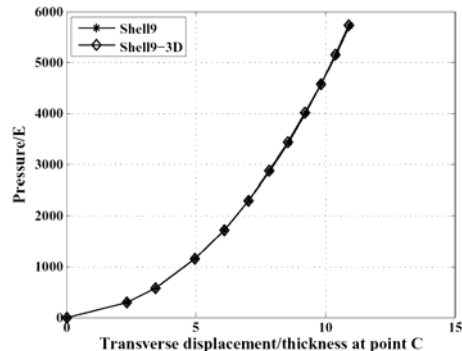


Figure 6: Pressure/E vs. transverse displacement/thickness at point C for $L/t=10000$

3.2 A clamped square plate under uniform pressure

The clamped square plate in Fig. 2 is revisited. The length L of the plate is 2" and the thickness t is 0.02". The plate is subjected to transverse uniform pressure. Geometrically nonlinear analysis is carried out using both the SHELL9-3D element

and the SHELL9 element. The results of the geometrically nonlinear analysis are shown in Fig. 4 where the solution obtained by the SHELL9-3D element is almost identical to that by the SHELL9 element.

Subsequently, two plates with the thickness equal to 0.002" and 0.0002" are considered. The results of geometrically nonlinear analysis are shown in Fig. 5 and Fig. 6, demonstrating that performance of the SHELL9-3D element is comparable with that of the SHELL9 element.

3.3 A circular ring under line loads

A circular ring, subjected to two opposite line loads, as shown in Fig. 7, serves as a simple example problem to examine the membrane locking of curved shell elements.

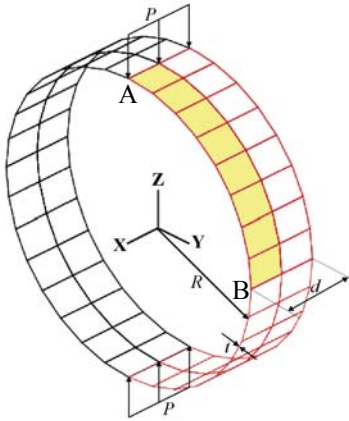


Figure 7: A circular ring subjected to line loads

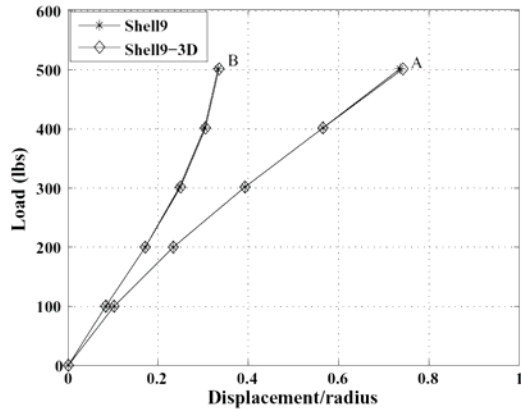


Figure 8: Load vs. displacement/radius at point A and B for the pinched ring

The radius R of the ring is 100" and the width d is 1". The ring material is isotropic with a Young's modulus $E = 1 \times 10^7$ psi and a Poisson's ratio $\nu = 0.3$. Due to the symmetry in geometry and loading conditions, only one quarter in the circumferential direction and one half in the width direction is modeled with an 1×4 uniform mesh. A geometrically nonlinear analysis is conducted for the radius-to-thickness ratios of $R/t = 100$. Figure 8 shows the displacement in the direction normal to the surface at two points. As shown in the figure, there is no difference between the SHELL9 and SHELL9-3D solutions. Both elements perform well, exhibiting no signs of element locking. Deformed shapes of the pinched ring are shown in Fig. 9.

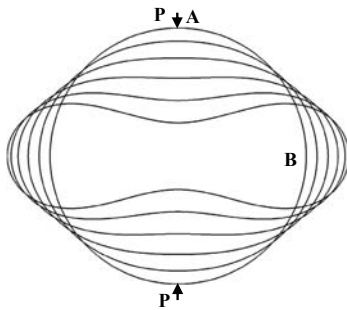


Figure 9: Undeformed and deformed configurations of the pinched ring for $P=0, 100, 200, 300, 400$ and 500 (lbs)

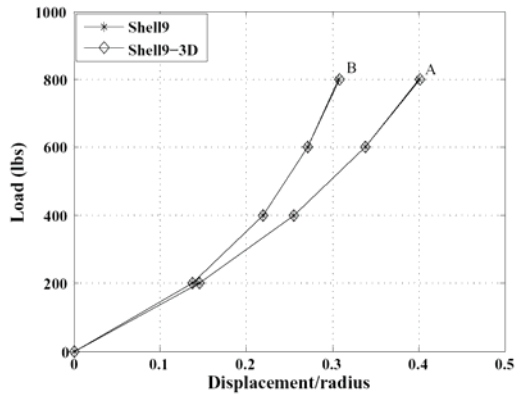


Figure 10: Load vs. displacement/radius at point A and B for the pulled ring

Subsequently, the ring subjected to the line loads in the opposite direction is considered. The results of geometrically nonlinear analysis are shown in Fig. 10, where solutions obtained by using the SHELL9 element and the SHELL9-3D element are almost identical. Deformed configurations of the pulled ring are shown in Fig. 11.

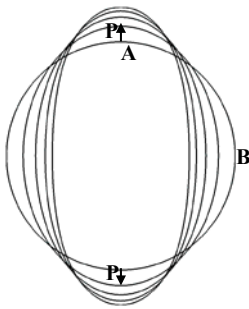


Figure 11: Undeformed and deformed configurations of the pulled ring for $P = 0, 200, 400, 600, 800$ (lbs)

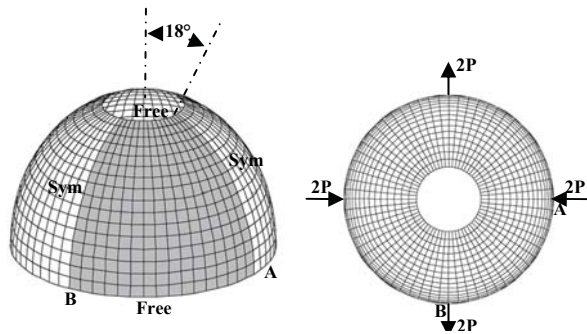


Figure 12: A hemisphere subjected to alternating point loads

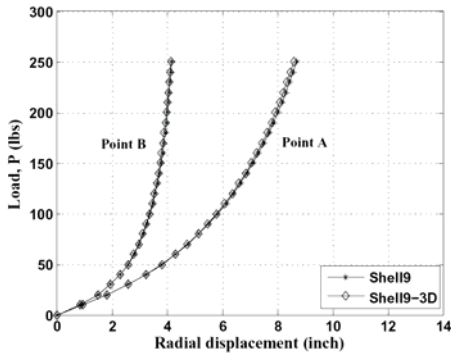


Figure 13: Load vs. radial displacement at point A and B for the cut-out hemisphere

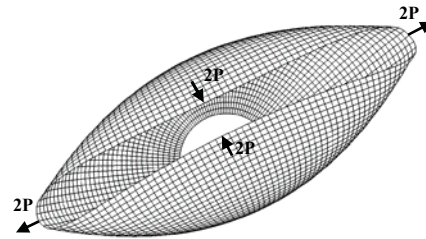


Figure 14: Deformed configuration of the cut-out hemisphere for $P = 250$ (lbs)

3.4 A cut-out hemisphere subjected to alternating point loads

A hemispherical shell with an eighteen-degree hole cut-out is subjected to alternating point loads as shown in Fig 12. The radius R of the hemisphere is 10" and the thickness t is 0.04". The hemisphere material is isotropic with a Young's modulus $E = 6.825 \times 10^7$ psi and a Poisson's ratio $\nu = 0.3$. Due to the symmetry in geometry and loading conditions, only one quarter is modeled with an 8×8 uniform mesh. A geometrically nonlinear analysis is conducted using the SHELL9 element and the SHELL9-3D element. Figure 13 shows the displacement in the direction normal to the surface at the two points. As shown in the figure, there is no difference between the SHELL9 and SHELL9-3D solutions. Both elements perform well, exhibiting no signs of element locking. Figure 14 shows a deformed configuration of the hemisphere for $P=250$ (lbs).

4 Conclusions

The results of numerical tests, conducted on geometrically nonlinear plates and shells, demonstrate the validity and the effectiveness of the newly developed solid shell element with quadratic displacement through the thickness. For the cases involving linear elastic material, the differences between the SHELL9 element with linear displacement through the thickness and the SHELL-3D element with quadratic displacement through the thickness are negligible. For the SHELL9-3D element, the nodal degrees of freedom associated with the quadratic terms in the assumed displacement through the thickness are statically condensed out at the

element level with the understanding that the strain energy associated with these degrees of freedom is negligible. Accordingly, the present approach does not introduce any additional degrees of freedom at the global level.

It is to be noted that the effectiveness of the present solid shell approach which allows direct use of the 3D constitutive equations can be appreciated only when it is applied to analysis of nonlinear shells such as elastoplastic shells using the full Newton-Raphson iteration with the tangent stiffness matrix. For shells of linear elastic materials, it is adequate to use an element such as the SHELL9 with the linear displacement through thickness in conjunction with the modified constitutive equation. It remains to be seen how the present approach will fare in comparison with other formulations reported in the literature that also allow 3D constitutive equations.

Acknowledgement: The authors would like to thank Dr. Yapa Rajapakse at the Office of Naval Research for the support of this work.

References

Atluri, S.N.; Zhu, T. (1998): A new Meshless Local Petrov-Galerkin (MLPG) approach in computational mechanics, *Computational Mechanics*, Vol. 22, pp. 117-127

Ahmad, S.; Irons, B.M.; Zienkiewicz, O.C. (1970): Analysis of thick and thin shell structures by curved elements, *Int. J. Numer. Meth. Engng*, Vol. 2, pp. 419-451

Arciniega, R.A.; Reddy, J.N. (2007): Tensor-based finite element formulation for geometrically nonlinear analysis of shell structures, *Comput. Methods Appl. Mech. Engrg.*, Vol. 196, pp. 1048-1073

Ausserer, M.F.; Lee, S.W. (1988): An eighteen node solid element for thin shell analysis, *Int. J. Numer. Meth. Engng*, Vol. 26, pp. 1345-1364

Balah, M.; Al-Ghamedy, H.N. (2002): Finite element formulation of a third order laminated finite rotation shell element, *Computers and Structures*, Vol. 80, pp. 1975-1990

Basar, Y.; Hanskotter, U.; Schwab, Ch. (2003), A general high-order finite element formulation for shells at large strains and finite rotations, *Int. J. Numer. Meth. Engng*, Vol. 57, pp. 2147-2175

El-Abbasi, N.; Meguid, S.A. (2000): A new shell element accounting for through-thickness deformation, *Comput. Methods Appl. Mech. Engrg.*, Vol. 189, pp. 841-862

- Han, Z.D.; Rajendran, A.M.; Atluri, S.N.** (2005): Meshless Local Petrov-Galerkin (MLPG) approaches for solving nonlinear problems with large deformations and rotations, *CMES: Computer Modeling in Engineering & Sciences*, Vol. 10, no. 1, pp. 1-12.
- Hauptmann R.; Schweizerhof K.** (1998): A systematic development of 'solid-shell' element formulations for linear and non-linear analyses employing only displacement degrees of freedom, *Int. J. Numer. Meth. Engng.*, Vol. 42, pp. 49-69
- Jarak, T.; Soric, J.; Hoster, J.** (2007): Analysis of shell deformation responses by the Meshless Local Petrov-Galerkin (MLPG) approach, *CMES: Computer Modeling in Engineering & Sciences*, Vol. 18, no. 3, pp. 235-246
- Kim, Y.H.; Lee, S.W.** (1988): A solid element formulation for large deflection analysis of composite shell structures, *Computers and Structures*, Vol. 30, pp. 269-274
- Klinkel, S.; Gruttmann, F.; Wagner, W.** (2006): A robust non-linear solid shell element based on a mixed variational formulation, *Comput. Methods Appl. Mech. Engrg.*, Vol 195, pp. 179-201
- Kulikov, G.M.; Plotnikova, S.V.** (2008): Finite rotation geometrically exact four-node solid-shell element with seven displacement degrees of freedom, *CMES: Computer Modeling in Engineering & Sciences*, Vol. 28, no 1., pp. 15-38
- Lee, K.; Cho, C.M.; Lee, S.W.** (2002): A geometrically nonlinear nine-node solid shell element formulation with reduced sensitivity to mesh distortion, *CMES: Computer Modeling in Engineering & Sciences*, Vol. 3, no 3., pp. 339-349
- Lee, K.; Lee, S.W.** (2001): Advances in the assumed strain formulation for solid shell elements, 6th USNCCM, Dearborn, MI, August 1-3
- Lee, S.W.; Pian, T.H.H.** (1978): Improvements of Plate and Shell Finite Elements by Mixed Formulations, *AIAA Journal*, Vol. 16, No 1, pp. 29-34
- Li, Q.; Soric J.; Jarak, T.; Atluri, S.N.** (2005): A locking-free Meshless Local Petrov-Galerkin formulation for thick and thin plates, *Journal of Computational Physics*, vol. 208, pp. 116-133.
- Liu, C.** (2005): Computational applications of the poincare group on the elasto-plasticity with kinematic hardening, *CMES: Computer Modeling in Engineering & Sciences*, Vol. 8, no. 3, pp. 231-258.
- Parisch, H.** (1995): A continuum-based shell theory for non-linear applications, *Int. J. Numer. Meth. Engng*, Vol. 38, pp. 1855-1883
- Park, H.C.; Cho, C.M.; Lee, S.W.** (1995): An efficient assumed strain element model with six DOF per node for geometrically nonlinear shells, *Int. J. Numer. Meth. Engng*, Vol. 38, pp. 4101-4122

Park, H.C.; Lee, S.W. (1995): A local coordinate system for assumed strain shell element formulation, *Computational Mechanics*, Vol. 15, No. 5, pp. 473-484

Rhiu, J.J.; Lee, S.W. (1987): A new efficient mixed formulation for thin shell finite element model, *Int. J. Numer. Meth. Engng*, Vol. 24, pp. 581-604

Sansour, C (1995): A theory and finite element formulation of shells at finite deformations involving thickness change: circumventing the use of a rotation tensor, *Archive of Applied Mechanics*, Vol. 65, pp. 194-216

Simo, J.C.; Rifai, M.S. (1990): On a stress resultant geometrically exact shell model. part III: computational aspects of the nonlinear theory, *Comp. Meth. Appl. Mech. Eng.*, Vol. 79, pp. 21-70

Sladek, J.; Sladek, V.; Wen, P.H.; Aliabadi, M.H. (2006): Meshless Local Petrov-Galerkin (MLPG) Method for shear deformable shells analysis, *CMES: Computer Modeling in Engineering & Sciences*, Vol. 6, no. 2, pp. 103-117

Soric J.; Li, Q.; Jarak, T.; Atluri, S.N. (2004): Meshless Local Petrov-Galerkin (MLPG) formulation for analysis of thick plates, *CMES: Computer Modeling in Engineering & Sciences*, vol. 6, no. 4, pp. 349-357.

Tabiei, A.; Tanov, R. (2000): A nonlinear higher order shear deformation shell element for dynamic explicit analysis: Part I. Formulation and finite element equations, *Finite Elements in Analysis and Design*, Vol. 36, pp. 17-37

Tonkovic, Z.; Soric, J.; Skozrit, I. (2008): On numerical modeling of cyclic elastoplastic response of shell structures, *CMES: Computer Modeling in Engineering & Sciences*, Vol. 26, no. 2, pp. 75-90

Vu-Quoc, L.; Tan, X.G (2003): Optimal solid shells for non-linear analyses of multilayer composites. I. Statics, *Comput. Methods Appl. Mech. Engrg.*, Vol. 192, pp. 975-1016

Yang, H.T.Y.; Saigal, S.; Masoud, A.; Kapania, R.K. (2000): A survey of recent shell finite elements, *Int. J. Numer. Meth. Engng*, Vol. 47, 2000, pp. 101-127